

Joint User Priority and Power Scheduling for QoS-Aware WMMSE Precoding: A Constrained-Actor Attentive-Critic Approach

Kexuan Wang and An Liu, *Senior Member, IEEE*

Abstract—6G wireless networks are expected to support diverse quality-of-service (QoS) demands while maintaining high energy efficiency. Weighted Minimum Mean Square Error (WMMSE) precoding with fixed user priorities and transmit power is widely recognized for enhancing overall system performance but lacks flexibility to adapt to user-specific QoS requirements and time-varying channel conditions. To address this, we propose a novel constrained reinforcement learning (CRL) algorithm, Constrained-Actor Attentive-Critic (CAAC), which uses a policy network to dynamically allocate user priorities and power for WMMSE precoding. Specifically, CAAC integrates a Constrained Stochastic Successive Convex Approximation (CSSCA) method to optimize the policy, enabling more effective handling of energy efficiency goals and satisfaction of stochastic non-convex QoS constraints compared to traditional and existing CRL methods. Moreover, CAAC employs lightweight attention-enhanced Q-networks to evaluate policy updates without prior environment model knowledge. The network architecture not only enhances representational capacity but also boosts learning efficiency. Simulation results show that CAAC outperforms baselines in both energy efficiency and QoS satisfaction.

Index Terms—Radio resource allocation, WMMSE, CRL.

I. INTRODUCTION

With the rise of diverse applications, 6G networks are expected to efficiently support heterogeneous quality-of-service (QoS) requirements. For example, delay-sensitive applications such as autonomous driving and virtual reality require low-latency transmission for safety and/or immersive experiences, while delay-tolerant applications like web browsing prioritize high transmission rates [1]. Meanwhile, power consumption has also become a critical concern amid the rapid growth of connected devices and rising environmental pressures [2].

Weighted Minimum Mean Square Error (WMMSE) is a widely studied technique enabling MIMO systems to achieve near-optimal throughput, thus improving overall communication quality [3]. To enhance its practicality, low-complexity and robust variants were proposed in [4] and [5]. However, these methods typically adopt fixed user priorities and transmit power, neglecting user-specific QoS requirements and power consumption concerns. Using traditional iterative optimization methods to address the user priority and transmit power scheduling (UPTPS) problem would require perfect foresight of future channel and data traffic, which is unrealistic in highly dynamic environments. Heuristic approaches in [6] and [7] mitigate this by prioritizing users with large queues or low past rates, but lack robustness due to missing theoretical guarantees.

Recently, [8]–[10] modeled radio resource scheduling problems with QoS constraints as Constrained Markov Decision Processes (CMDPs) and addressed them via Actor-Critic-based constrained reinforcement learning (CRL). Their Actor module optimizes the scheduling policy by solving the CMDP, while their Critic module evaluates policy updates in terms of improving the objective and satisfying the constraints, ultimately finding a good trade-off between the two without requiring any environment model knowledge. However, in the case of UPTPS for WMMSE precoding, the WMMSE precoding process introduces significant non-convexity into both the objective function and the QoS constraints, making it difficult for these methods to guarantee a feasible solution. Specifically, most existing CRL algorithms are designed for simpler constraints. For example, the widely used trust region policy optimization-Lagrangian (TRPO-Lag) and proximal policy optimization-Lagrangian (PPO-Lag) [11] transform CMDPs into max-min saddle-point problems and address them by stochastic gradient descent, which are only suitable for constraints with deterministic convex feasible sets. The constrained Policy Optimization (CPO) algorithm [12] employs approximate operations to construct convex surrogate problems with acceptable computational overhead, which also cannot guarantee a feasible final solution. Moreover, as the number of users increases, the number of Q-networks grows rapidly, resulting in high training overhead and slower convergence. Existing methods have largely overlooked scalability designs for this issue. Our previously proposed successive convex approximation-based off-policy optimization (SCAOP) algorithm [13] considers the non-convexity in policy optimization and employs a simple Monte Carlo (MC) method to avoid Q-networks. However, its performance degrades with insufficient samples due to inaccurate evaluation.

To tackle these challenges, we propose a novel Constrained-Actor Attentive-Critic (CAAC) algorithm to dynamically schedule user priorities and transmit power for WMMSE. Compared to existing CRL algorithms, CAAC introduces two key improvements: 1) the Actor module optimizes scheduling policy by a constrained stochastic successive convex approximation (CSSCA) method, which can reduce power consumption while effectively satisfying stochastic non-convex QoS constraints by solving a sequence of convex surrogate problems; 2) the Critic module employs a lightweight attention-enhanced Q-network architecture, which significantly improves the training efficiency and policy evaluation performance. Simulation results show that CAAC outperforms baseline algorithms in both energy efficiency and QoS guarantee.

Kexuan Wang and An Liu are with the College of Information Science and Electronic Engineering, Zhejiang University, Hangzhou 310027, China (email: {kexuanWang, anliu}@zju.edu.cn). (*Corresponding Author: An Liu*)

II. SYSTEM MODEL AND PROBLEM FORMULATION

A. System Model

This section considers a MIMO system comprising a base station (BS) equipped with M antennas and K single-antenna users, as depicted in Fig. 1, where the users are indexed by the set $\mathcal{K} = \{1, \dots, K\}$. The time dimension is divided into timeslots of duration τ , each indexed by t . Moreover, the channel from BS to the k -th user is denoted by $\mathbf{h}_{k,t} \in \mathbb{C}^{1 \times M}, \forall t$.

We now introduce the downlink transmission process. At each timeslot t , bursty data of length $A_{k,t}$ is generated with probability P_k and stored in a dedicated buffer for user k , along with any previously untransmitted data. Specifically, the queue length is updated according to

$$L_{k,t} = L_{k,t-1} - R_{k,t-1}\tau + A_{k,t}, \forall k, t,$$

where $R_{k,t-1}$ is the downlink transmission rate for user k at timeslot $t-1$. Based on the current channel conditions and data queue states, the BS assigns user priority weights $\boldsymbol{\omega}_t \triangleq \{\omega_{k,t}\}_{k \in \mathcal{K}}$ and the total transmit power p_t , and then executes the WMMSE precoding [3]. Then, the obtained precoder vector $\mathbf{v}_{k,t}$ is used to process the transmit signal $s_{k,t}$ for user k , where $\sum_{k=1}^K \text{Tr}(\mathbf{v}_{k,t}^H \mathbf{v}_{k,t}) = p_t$ and $|s_{k,t}| = 1$. Further, the received signal $y_{k,t} \in \mathbb{C}$ at user k is given by

$$y_{k,t} = \mathbf{h}_{k,t} \mathbf{v}_{k,t} s_{k,t} + \sum_{m \neq k} \mathbf{h}_{k,t} \mathbf{v}_{m,t} s_{m,t} + n_k, \forall k, t$$

where $n_k \sim \mathcal{CN}(0, \sigma_k^2)$ represents the additive white Gaussian noise. Finally, the downlink transmission rate for user k at the current timeslot t is expressed as

$$R_{k,t} = W \log_2 \left(1 + \frac{|(\mathbf{h}_{k,t})^H \mathbf{v}_{k,t}|^2}{\sum_{m \neq k} |(\mathbf{h}_{k,t})^H \mathbf{v}_{m,t}|^2 + \sigma_k^2} \right),$$

where W denotes the bandwidth.

B. Problem Formulation

This paper aims to find the optimal UPTPS for WMMSE precoding, which minimizes the system energy consumption under heterogeneous QoS constraints. This can be formulated as the following sequential decision-making problem:

$$\begin{aligned} & \max_{\{\boldsymbol{\omega}_t, p_t\}_{t=0,1,\dots}} \lim_{T \rightarrow \infty} \frac{1}{T} \mathbb{E} \left[\sum_{t=0}^{T-1} p_t \right] \\ & \text{s.t.} \lim_{T \rightarrow \infty} \frac{1}{T} \mathbb{E} \left[\sum_{t=0}^{T-1} \sum_{n=1}^N \delta(n - \varrho_k) \mathbb{U}(n, k, t) \right] \leq c_k, \forall k. \end{aligned} \quad (1)$$

where $\mathbb{E}[\cdot]$ is the expectation taken over channel fading distributions and data arrival processes, ϱ_k represents the QoS category required by user k , $\delta(\cdot)$ is discrete impulse response function, $\mathbb{U}(n, k, t)$ denotes the utility function corresponding to the n -th QoS type, and $c_{b,k}$ denotes the minimum QoS threshold acceptable for user k .

To accommodate diverse applications, the system is required to support $N \geq 1$ types of QoS demands. This paper considers two type of QoS requirements as representative examples: 1) If the k -th user is delay-sensitive, we define the utility function $\mathbb{U}(1, k, t) = L_{k,t}/a_k$, where $a_k = P_{k,t} \mathbb{E}[A_{k,t}]$ denotes the

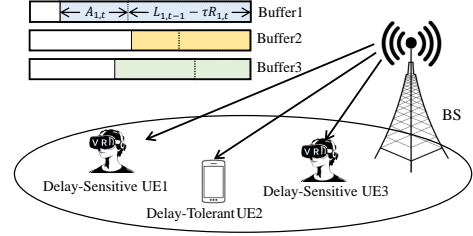


Figure 1. Downlink transmission with heterogeneous QoS support.

average data arrival per timeslot for user k ; 2) If the k -th user is delay-tolerant, the utility function is defined as $\mathbb{U}(2, k, t) = -\mathcal{R}_{k,t}$. It is worth noting that additional QoS requirements of practical interest can also be incorporated by redefining the corresponding utility functions $\mathbb{U}(n, k, t)$, without requiring any modification to the proposed algorithm.

III. THE CONSTRAINED-ACTOR ATTENTIVE-CRITIC ALGORITHM DESIGN

A. Constrained Markov Decision Process

To facilitate tractable analysis, we model the original problem (1) as a Constrained Markov Decision Process (CMDP), represented by a tuple $(\mathcal{S}, \mathcal{A}, P, R, C)$, where:

- **The state space \mathcal{S} :** the state at timeslot t is $\mathbf{s}_t \triangleq \{\mathbf{L}_t; \mathbf{H}_t\}$, where $\mathbf{L}_t \triangleq [L_{1,t}, L_{2,t}, \dots, L_{K,t}]^T$ denotes the queue length vector, and $\mathbf{H}_t \triangleq [\mathbf{h}_{1,t}, \mathbf{h}_{2,t}, \dots, \mathbf{h}_{K,t}]^T$ is the channel state information (CSI). Accordingly, the state space \mathcal{S} is defined as the Cartesian product of the queue length space \mathbb{R}_+^K and the CSI space $\mathbb{C}^{K \times M}$.
- **The action space \mathcal{A} :** the action $\mathbf{a}_t \triangleq \{\boldsymbol{\omega}_t, p_t\}$ is sampled from the action space \mathcal{A} according to a policy $\pi: \mathcal{S} \rightarrow \mathbf{P}(\mathcal{A})$, where $\pi(\mathbf{a}_t | \mathbf{s}_t)$ denoting the probability of selecting \mathbf{a}_t given state \mathbf{s}_t . To mitigate the curse of dimensionality, the policy π is parameterized by deep neural networks (DNNs), and is further denoted by π_θ .
- **The transition probability function P :** the environment evolves according to an unknown transition probability function $P: \mathcal{S} \times \mathcal{A} \times \mathcal{S} \rightarrow [0, 1]$, where $P(\mathbf{s}_{t+1} | \mathbf{s}_t, \mathbf{a}_t)$ denotes the probability of reaching state \mathbf{s}_{t+1} from \mathbf{s}_t given action \mathbf{a}_t . Together, the function P and policy π_θ determine a trajectory distribution σ_π , i.e., $\mathbf{s}_t \sim P(\cdot | \mathbf{s}_{t-1}, \mathbf{a}_{t-1}), \mathbf{a}_t \sim \pi_\theta(\cdot | \mathbf{s}_t)$.
- **Reward function R and C :** after taking action \mathbf{a}_t , the agent (BS) obtains a system throughput-related reward $R(\mathbf{s}_t, \mathbf{a}_t) \triangleq p_t$, and some QoS-related rewards $C_k(\mathbf{s}_t, \mathbf{a}_t) \triangleq \sum_{n=1}^N \delta(n - \varrho_k) \mathbb{U}(n, k, t)$.

Accordingly, the original problem (1) can be reformulated as:

$$\begin{aligned} & \min_{\boldsymbol{\theta} \in \Theta} f_0(\boldsymbol{\theta}) \triangleq \lim_{T \rightarrow \infty} \frac{1}{T} \mathbb{E}_{p_{\pi_\theta}} \left[\sum_{t=0}^{T-1} C'_0(\mathbf{s}_t, \mathbf{a}_t) \right] \\ & \text{s.t.} f_k(\boldsymbol{\theta}) \triangleq \lim_{T \rightarrow \infty} \frac{1}{T} \mathbb{E}_{p_{\pi_\theta}} \left[\sum_{t=0}^{T-1} C'_k(\mathbf{s}_t, \mathbf{a}_t) \right] \leq 0, \forall k, \end{aligned} \quad (2)$$

where $C'_0(\mathbf{s}_t, \mathbf{a}_t) = R(\mathbf{s}_t, \mathbf{a}_t)$ and $C'_k(\mathbf{s}_t, \mathbf{a}_t) = C_k(\mathbf{s}_t, \mathbf{a}_t) - c_k, k = 1, 2, \dots, K$. In the following, we propose the Constrained-Actor Attentive-Critic (CAAC) algorithm, which alternates between Actor and Critic modules to solve

Algorithm 1 Constrained-Actor Attentive-Critic Algorithm

Input: The initial entries of $\kappa_1, \kappa_2, \kappa_3, \omega_0$ and θ_0 .

for $t = 0, 1, 2 \dots$

 Sample the new observation $\tilde{\varepsilon}_t$ and update the set ε_i .

The Critic Module:

 Calculate $G_{i,t}^B$ and update ω^i by (13) for T_{cri} times.

The Actor Module:

 Estimate $\hat{f}_{k,i}$ and $\hat{g}_{k,i}$ according to (3)-(6).

 Update the surrogate function $\{\tilde{f}_{k,t}(\theta)\}_{k=0,\dots,K}$ via (7).

if Problem (8) is feasible: Solve (8) to obtain θ_t .

else: Solve (9) to obtain $\bar{\theta}_t$. (*Feasible update*)

 Update policy parameters θ_{t+1} according to (10).

this CMDP. The algorithm design is detailed below, with the overall procedure summarized in Algorithm 1.

B. The Actor Module

The Actor module executes the policy network and optimizes it using CSSCA method. CSSCA estimates the values and gradients of the objective and constraint functions through interactions with the environment, and then handle the non-convex CMDP by solving a sequence of convex quadratic optimization problems constructed from these estimates.

At the beginning of the i -th policy update, the policy π_{θ_i} interacts with the environment B times, collecting an observation set $\varepsilon_i = \{\tilde{\varepsilon}_t\}_{t=B(i-1)+1:B(i)}$, where each tuple is given by $\tilde{\varepsilon}_t \triangleq \{s_t, \mathbf{a}_t, \{C'_l(s_t, \mathbf{a}_t)\}_{l=0,\dots,L}, s_{t+1}\}$. These tuples are stored in a replay buffer for function and gradient estimation. Specifically, first apply the sample average approximation (SAA) method to compute sample-based estimates of the objective and constraint functions:

$$\tilde{f}_{k,i} = \hat{\mathbb{E}}_{\varepsilon_i} [C'_{k,t}], \forall k, t. \quad (3)$$

where $\hat{\mathbb{E}}_{\varepsilon_i}$ denotes the empirical mean over the observation set ε_i . Moreover, according to the policy gradient theorem [13], the gradient $\nabla f_k(\theta)$ is expressed as

$$\nabla f_{k,i}(\theta) = \mathbb{E} [Q_k^{\pi_{\theta_i}}(s, \mathbf{a}) \nabla_{\theta} \log \pi_{\theta_i}(\mathbf{a} | s)], \forall k,$$

where $\{Q_k^{\pi_{\theta_i}}\}_{k=0,\dots,K}$ serve as crucial tools for assessing the effectiveness of the current policy in improving system throughput or satisfying QoS constraints, and are defined as

$$Q_k^{\pi_{\theta_i}}(s, \mathbf{a}) = \mathbb{E} \left[\sum_{l=0}^{\infty} (C'_{k,l} - f_k(\theta_i)) | s_0, \mathbf{a}_0 = s, \mathbf{a} \right].$$

These Q-functions are approximated by Q-networks $\{Q_k^{\omega_i}\}_{k=0,\dots,K}$ in the Critic module. Similarly, following the SAA, the sample-based policy gradients are estimated as

$$\tilde{g}_{k,i} = \hat{\mathbb{E}}_{\varepsilon_i} [Q_k^{\omega_i}(s, \mathbf{a}) \nabla_{\theta} \log \pi_{\theta_i}(\mathbf{a} | s)], \forall k. \quad (4)$$

To stabilize the learning process, we apply recursive updates to the function and gradient estimates as follows:

$$\hat{f}_{k,i+1} = (1 - \eta_{i+1}) \hat{f}_{k,i} + \eta_{i+1} \tilde{f}_{k,i}, \forall k, i, \quad (5)$$

$$\hat{g}_{k,i+1} = (1 - \eta_{i+1}) \hat{g}_{k,i} + \eta_{i+1} \tilde{g}_{k,i}, \forall k, i, \quad (6)$$

where $\eta_i \triangleq (i+1)^{-\kappa_1}$ and $\kappa_1 \in (0, 1)$.

Using $\hat{f}_{k,i}$ and $\hat{g}_{k,i}$, we construct convex quadratic surrogate functions for the objective/constraint functions as follows:

$$\tilde{f}_{k,i}(\theta) = \hat{f}_{k,i} + (\hat{g}_{k,i})^\top (\theta - \theta_i) + \zeta_k \|\theta - \theta_i\|_2^2, \forall k \quad (7)$$

where $\zeta_k > 0$ is a constant. The policy update is then carried out by solving the following objective optimization problem:

$$\bar{\theta}_i = \underset{\theta \in \Theta}{\operatorname{argmin}} \tilde{f}_{0,i}(\theta) \quad \text{s.t.} \quad \tilde{f}_{k,i}(\theta) \leq 0, \forall k. \quad (8)$$

If it is infeasible, we solve a feasible optimization problem:

$$\bar{\theta}_i = \underset{\theta \in \Theta, y}{\operatorname{argmin}} \alpha \quad \text{s.t.} \quad \tilde{f}_{k,i}(\theta) \leq \alpha, \forall k. \quad (9)$$

Both (8) and (9) can be easily solved by standard convex optimization algorithms, e.g. Lagrange-dual methods. Finally, the policy parameters are updated via:

$$\theta_i = (1 - \mu_i) \theta_{i-1} + \mu_i \bar{\theta}_i. \quad (10)$$

where $\mu_i \triangleq (i+1)^{-\kappa_2}$ and $\kappa_2 \in (0, 1)$.

C. The Critic Module

The Critic module aims to train Q-networks $\{Q_k^{\omega_i}\}_{k=0,\dots,K}$ to approximate Q-functions $\{Q_k^{\pi_{\theta_i}}\}_{k=0,\dots,K}$.

1) *Lightweight Attention-Enhanced Q-Networks:* As shown in Fig. 2, we design a lightweight attention-enhanced architecture for Q-networks, comprising three main components:

- **A Shared Embedding Layer:** The embedding layer is composed of a set of embedding functions $\{g_k(\cdot)\}_{k=1:K}$, which are shared across all Q-networks. We decompose the state s_t and priority weights ω_t into some user-specific tuples $\{o_{k,t} \triangleq (L_{k,t}, h_{k,t}, \omega_{k,t})\}_{k=1}^K$. Each tuple $o_{k,t}$ can be encoded into a low-dimensional embedding vector $e_{k,t} \triangleq g_k(o_{k,t})$ through $g_k(\cdot)$.
- **A Shared Attention Layer:** Considering that the QoS performance of a user k is primarily determined by the action \mathbf{a}_t and its own state $o_{k,t}$, but may also be affected by neighboring users to varying degrees, we construct a feature vector $\mathbf{x}_{k,t}$ for each Q-network k as follows:

$$\mathbf{x}_{k,t} = \mathbf{a}_t \oplus \mathbf{v}_{k,t} \oplus \sum_{k' \in \mathcal{K}/k} \alpha_{k,k',t} \mathbf{v}_{k',t}, \quad (11)$$

where the value vector $\mathbf{v}_{k',t} = \mathbf{W}^V e_{k',t}$ is a linear projection of $e_{k',t}$, $\alpha_{k,k',t}$ denotes the attention weight, and \oplus denotes vector concatenation. For any $k \in \mathcal{K}$, the attention weight $\alpha_{k,k',t}$ is computed according to

$$\alpha_{k,k',t} = \operatorname{softmax}((\mathbf{k}_{k,t})^T \mathbf{q}_{k',t}), \quad (12)$$

where $\mathbf{k}_{k,t} \triangleq \mathbf{W}^K e_{k,t}$ and $\mathbf{q}_{k',t} \triangleq \mathbf{W}^Q e_{k',t}$ are the key and query vectors obtained via linear transformations. The inner product $(\mathbf{k}_{k,t})^T \mathbf{q}_{k',t}$ reflects the relevance between user k' state and user k' state. The parameter matrices $\mathbf{W}^K \in \mathbb{R}^{L_1 \times L_2/2}$, $\mathbf{W}^Q \in \mathbb{R}^{L_1 \times L_2/2}$, and $\mathbf{W}^V \in \mathbb{R}^{L_1 \times L_2/2}$ are shared across all Q-networks. In the case of $k = 0$, $\mathbf{v}_{k,t}$ degenerates into an empty vector, and the attention weights are set uniformly (i.e., $\alpha_{0,k',t} = 1$), i.e., the Q-network corresponding to objective function equally attends to each user' state.

- **Separate Output Functions:** Finally, each $\mathbf{x}_{k,t}$ is passed through a separate output function $f_k(\cdot)$, a two-layer fully connected network (FCN), to produce $Q_k^{\omega_i}(s_t, \mathbf{a}_t)$.

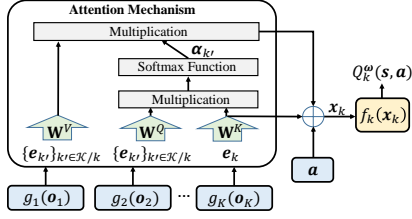


Figure 2. The lightweight attention-enhanced Q-network architecture.

Conventional Actor-Critic-based CRL typically uses independent Q-networks for each Q-function. In contrast, Q-networks in this work adopts shared embedding and attention layers, reducing the parameter size and improving training efficiency. Since all users share the same structure of state information, this shared design encourages a common embedding space, thereby enhancing generalization. Moreover, the attention mechanism enables Q-networks to focus on critical information, boosting their representational capacity.

2) *The training for Q-networks:* Then, the Q-networks $\{Q_k^{\omega_i}\}_{k=0, \dots, K}$ are optimized according to the classical temporal-difference (TD)-learning method [14], which minimizes the Bellman error of the Q-networks:

$$\mathcal{B}_k^{\omega_i}(s_t, \mathbf{a}_t, s_{t+1}) = \sum_{k=0}^K |Q_k^{\omega_i}(s_t, \mathbf{a}_t) - \mathcal{T}Q_k^{\omega_i}(s_t, \mathbf{a}_t)|^2,$$

where \mathcal{T} is the Bellman operator defined as

$$\mathcal{T}Q_k^{\omega_i}(s_t, \mathbf{a}_t) = \mathbb{E} \left[Q_{\omega_{k,i}}(s_{t+1}, \mathbf{a}'_{t+1}) + C'_{k,t} \right] - f_k(\theta_i),$$

where \mathbf{a}'_{t+1} is the action chosen by π_{θ_i} at the next state s_{t+1} . Since it is unrealistic to obtain the accurate function value $f_k(\theta_i)$ online, we replace it by $\hat{f}_{k,i}$. We divide the new observation set ε_i into T_{cri} mini-batches (with $T_{\text{cri}} < B$, where B is the total number of new observation samples in ε_i), indexed by $[\varepsilon_i^1, \dots, \varepsilon_i^{T_{\text{cri}}}, \dots, \varepsilon_i^{T_{\text{cri}}}]$, and perform the following TD-updates for T_{cri} times:

$$\omega_i \leftarrow \omega_i - v_i \mathbf{G}_{i,t_{\text{cri}}}^{\mathcal{B}}, \forall k, t_{\text{cri}}, \quad (13)$$

where $\mathbf{G}_{i,t_{\text{cri}}}^{\mathcal{B}}$ is a stochastic gradient term of Bellman error:

$$\mathbf{G}_{i,t_{\text{cri}}}^{\mathcal{B}} = \sum_{t \in \varepsilon_i^{t_{\text{cri}}}} \left(Q_k^{\omega_i}(s_t, \mathbf{a}_t) - C'_{k,t} + \hat{f}_{k,i} - Q_{\omega_{k,i}}(s_{t+1}, \mathbf{a}'_{t+1}) \right) \nabla_{\omega} Q_k^{\omega_i}(s_t, \mathbf{a}_t), \forall k, \quad (14)$$

where the step size $v_i \triangleq (i+1)^{-\kappa_3}$ with $\kappa_3 \in (0, 1)$.

D. Convergence Analysis

According to our previous work [13, Lemma 3], the design of the step size η_i ensures that $\hat{f}_{k,i}$ asymptotically converges to $f_k(\theta_i)$. Then, the TD updates can ensure that the Q-networks accurately approximate the Q-functions, as long as the representations of the Q-networks are strong enough and both the sample size B and the number of TD updates T_{cri} are sufficiently large [14]. In this case, $\tilde{\mathbf{g}}_k^t$ is an unbiased estimation of $\nabla J_k(\theta_t)$, and $\hat{\mathbf{g}}_{k,i}$ can also asymptotically converge to $\nabla J_k(\theta_t)$, provided that the step size parameters satisfy $\kappa_1 < \kappa_2$ [13, Lemma 3]. As iterations proceed, the objective updates (8) make the value of the objective function increase continuously and finally achieve a stationary point of the original problem (2); the feasible updates (9) ensure

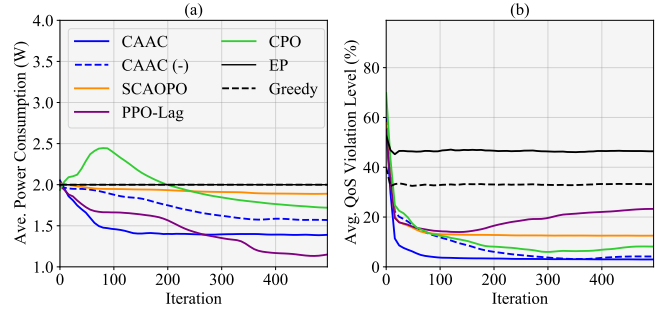


Figure 3. Convergence curves of algorithms.

the iteration point within or not far from the feasible QoS region, and asymptotically converges into the feasible QoS region almost surely. In practice, our lightweight network design enables the Q-networks to quickly converge to a small approximation error, thereby exhibiting good convergence performance despite the limited B and T_{cri} . This conclusion is also supported by simulation results in Section IV.

IV. NUMERICAL RESULTS

We consider a 500-meter radius cell with a BS equipped with $M = 16$ antennas serving $K \in \{4, 8, 12, 16\}$ single-antenna users. Each user moves in a random direction at 3 km/h and reverses direction at the cell boundary. The system operates at a carrier frequency of $f_0 = 3.5$ GHz with a timeslot duration of $\tau = 1$ ms, transmission bandwidth $W = 1$ MHz, and noise power density $\delta_0 = -174$ dBm/Hz. A block fading channel model $\mathbf{h}_{k,t} = \sqrt{\alpha_{k,t}} \tilde{\mathbf{h}}_{k,t}$ is used following [15], where $\alpha_{k,t} = 34 + 40 \log(d_k)$ models large-scale fading, and d_k is the distance between the BS and user k . Small-scale fading follows the Jakes model $\tilde{\mathbf{h}}_{k,t} = \rho \tilde{\mathbf{h}}_{k,t-t} + \sqrt{1 - \rho^2} \mathbf{u}_{k,t}$, where $\tilde{\mathbf{h}}_{k,0}$ and $\mathbf{u}_{k,t}$ are i.i.d. complex Gaussian variables with unit variance, and $\rho = J_0(2\pi f_d \tau)$ is the correlation coefficient with J_0 being the zeroth-order Bessel function and f_d the maximum Doppler frequency. Half of the users are delay-sensitive, with $P_k \in [0.4, 0.6]$ and $A_{k,t}$ sampled from distribution $P(A_{k,t} = x) = \frac{(A_{k,t})^x}{x!} e^{-\lambda_k}$, where $\lambda_k \in [5, 15]$ Kbits. The maximum acceptable average delay for them is assumed to be $c_{k,b} = 3$ timeslots. The remaining users are delay-tolerant, with a minimum transmission rate $c_{k,b} = 5$ Mbps. The policy employs a three-layer FCN with a hidden layer width of 256. The embedding and attention layers of Q-networks have output dimensions $L_1 K$ ($L_1 = 2$) and $L_2 = 64$, while the output functions' hidden layer has $L_3 = 32$ units. At each iteration, the agent collects $B = 200$ observations and updates Q-networks for $T_{\text{cri}} = 10$ times. Step sizes are $\alpha_t = \frac{1}{t^{0.6}}$, $\beta_t = \frac{1}{t^{0.7}}$, and $\gamma_t = \frac{1}{t^{0.3}}$. All results are averaged over 5 random seeds.

Fig. 3 and Fig. 4 show algorithms' convergence behavior under $K = 8$ and their average performance over 500 iterations with varying user numbers, respectively. Specifically, Fig. 3-a and Fig. 4-a depict the average power consumption, while Fig. 3-b and Fig. 4-b show the average QoS violation level across users, which is measured by $\text{QoS}_{\text{gap}}(i) = \frac{1}{KB(i+1)} \sum_{t=0}^{B(i+1)-1} \sum_{k=1}^K \left[\sum_{n=1}^N \delta(n - \rho_k) \mathcal{U}(n, k, t) - c_k \right]^+$, where $[\cdot]^+$ denotes the positive part operator. Baselines include

Table I
COMPARISON OF Q-NETWORK PARAMETER SIZES.

Algorithm	Parameterize Size
Lightweight Attention-enhanced networks	$O((2M+1)L_1K^2(K+1) + (L_1K+L_3)(L_2+K+1)(K+1) + L_3(K+1))$
four-layer fully connected networks	$O((2M+1)L_1K + \frac{3L_1L_2}{2} + (L_2+K+1)L_3(K+1) + L_3(K+1))$

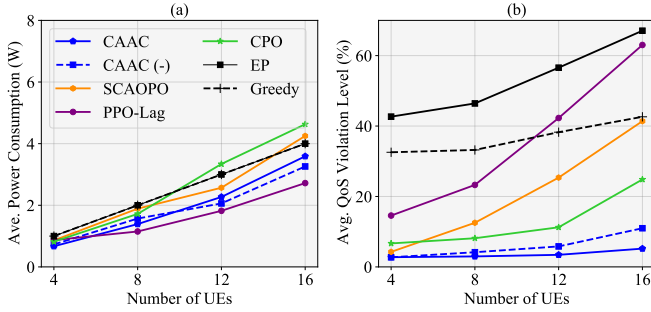


Figure 4. Performance versus the number of users.

configured power control schemes with equal-priority (EP) scheduling, a greedy priority scheduling that adjusts [6] using $QoS_{gap}(i)$ as priorities, and three advanced Actor-Critic-based CRL algorithms (PPO-Lag, CPO, and SCAOPO) introduced in Section I. We also design a CAAC variant, denoted as CAAC (-), by replacing the lightweight attention-enhanced Q-networks with separate four-layer FCNs, where the input and output dimensions of each layer in the latter match those of the former. As shown in Fig. 3, CAAC exhibits fast and stable convergence, reducing the average power consumption to 1.39 W and QoS violation level to 2.98%. The greedy method slightly outperforms the EP method, as it dynamically assigns higher priority weights to users with consistently poor performance. However, both methods are far from providing QoS guarantees to users, despite consuming more power than CRL-based algorithms. CPO and PPO-Lag demonstrate clear improvements over the greedy and EP methods. Nevertheless, as discussed in Section I, their policy optimization methods are not well-suited to handling non-convex objectives and constraints. As a result, CPO underperforms in power efficiency, while PPO-Lag struggles to meet QoS requirements effectively. SCAOPO, though effective in simpler scenarios in [13], performs unsatisfactorily in the more complex scenarios of this paper, as simple MC methods struggle to achieve accurate policy evaluation. CAAC converges significantly faster than CAAC (-), primarily because its parameter size is substantially smaller than that of CAAC (-), as compared in Table I. Moreover, CAAC achieves better final performance than CAAC (-), demonstrating that the integration of the attention mechanism enhances the representational capacity of the Q-networks. Fig. 4 shows CAAC consistently outperforms EP and greedy methods across all user scenarios. Although CRL-based algorithms perform similarly when there are fewer users, their performance gap with CAAC grows as the number of users increases. This is because large-scale user scenarios demand higher learning efficiency of Q-networks and make the problem (1) more non-convex, further amplifying the challenge for policy optimization. The advanced Q-network architecture and CSSCA-based policy optimization method are well-suited to address these requirements and challenges.

V. CONCLUSION

This paper proposes the CAAC algorithm for adaptive UPTPS in WMMSE precoding, aiming to minimize energy consumption while meeting heterogeneous QoS constraints. CAAC consists of an Actor module and a Critic module. The Actor executes the scheduling policy and optimizes it using a novel CSSCA method, which effectively handles non-convex stochastic objectives and QoS constraints. Meanwhile, the Critic evaluates the policy using lightweight attention-enhanced Q-networks, which are trained in a model-free manner and exhibit high learning efficiency. Simulation results demonstrate that CAAC offers superior energy efficiency and QoS satisfaction, making it a promising solution for green and intelligent resource allocation in future wireless systems.

REFERENCES

- [1] J. Tian, Q. Liu, H. Zhang, and D. Wu, "Multiagent deep-reinforcement-learning-based resource allocation for heterogeneous qos guarantees for vehicular networks," *IEEE Internet Things J.*, vol. 9, no. 3, pp. 1683–1695, 2021.
- [2] R. Deshpande, M. Katwe, K. Singh, M.-L. Ku, and D. Wing Kwan Ng, "Energy-efficient star-ris-aided mu-mimo for next-generation urllc systems," *IEEE Trans. Wireless Commun.*, vol. 23, no. 11, pp. 17807–17822, 2024.
- [3] X. Zhao, S. Lu, Q. Shi, and Z.-Q. Luo, "Rethinking WMMSE: Can its complexity scale linearly with the number of BS antennas?" *IEEE Trans. on Signal Process.*, vol. 71, pp. 433–446, 2023.
- [4] Q. Hu, Y. Cai, Q. Shi, K. Xu, G. Yu, and Z. Ding, "Iterative algorithm induced deep-unfolding neural networks: Precoding design for multiuser MIMO systems," *IEEE Trans. on Wireless Commun.*, vol. 20, no. 2, pp. 1394–1410, 2021.
- [5] K. Wang and A. Liu, "Robust wmmse-based precoder with practice-oriented design for massive mu-mimo," *IEEE Wireless Commun. Lett.*, vol. 13, no. 7, pp. 1858–1862, 2024.
- [6] G. Venkatraman, A. Tılli, J. Janhunen, and M. Juntti, "Low complexity multiuser mimo scheduling for weighted sum rate maximization," in *2014 22nd European Signal Processing Conference*, 2014, pp. 820–824.
- [7] A. Asadi and V. Mancuso, "A survey on opportunistic scheduling in wireless communications," *IEEE Commun. Surv. Tutor.*, vol. 15, no. 4, pp. 1671–1688, 2013.
- [8] M. Sulaiman, M. Ahmadi, M. A. Salahuddin, R. Boutaba, and A. Saleh, "Generalizable resource scaling of 5G slices using constrained reinforcement learning," in *Proc. NOMS IEEE/IFIP Netw. Operations Manage. Symp.* IEEE, 2023, pp. 1–9.
- [9] Y. Liu, J. Ding, Z.-L. Zhang, and X. Liu, "Clara: A constrained reinforcement learning based resource allocation framework for network slicing," in *2021 IEEE International Conference on Big Data (Big Data)*. IEEE, 2021, pp. 1427–1437.
- [10] Y. Huang, K. Chi, Q. Yang, Z. Yang, and Z. Zhang, "Soft actor-critic-based multi-user multi-tti mimo precoding in multi-modal real-time broadband communications," *IEEE Trans. Wireless Commun.*, vol. 23, no. 12, pp. 18286–18301, 2024.
- [11] A. Ray, J. Achiam, and D. Amodei, "Benchmarking safe exploration in deep reinforcement learning," *arXiv preprint arXiv:1910.01708*, vol. 7, no. 1, p. 2, 2019.
- [12] J. Achiam, D. Held, A. Tamar, and P. Abbeel, "Constrained policy optimization," in *ICML*. PMLR, 2017, pp. 22–31.
- [13] C. Tian, A. Liu, G. Huang, and W. Luo, "Successive convex approximation based off-policy optimization for constrained reinforcement learning," *IEEE Trans. Signal Process.*, vol. 70, pp. 1609–1624, 2022.
- [14] P. Xu and Q. Gu, "A finite-time analysis of Q-learning with neural network function approximation," in *ICML*, 2020, pp. 10555–10565.
- [15] Y. S. Nasir and D. Guo, "Multi-agent deep reinforcement learning for dynamic power allocation in wireless networks," *IEEE J. Sel. Areas Commun.*, vol. 37, no. 10, pp. 2239–2250, 2019.